Atomic Force Microscopic Imaging in Liquids: Effects of the Film Compressed between the Substrate and the Tip

E. F. de Souza,† R. A. Douglas, and O. Teschke*

Nano-structure Laboratory, Instituto de Fisica, Universidade Estadual de Campinas, 13081-970 Campinas SP, Brazil

Received June 11, 1997. In Final Form: August 25, 1997⊗

Measurements are made of the forces acting on the tip of an atomic force microscope when the sample and cantilever are in air and also immersed in polar solvents like water and DMSO. For large tip/substrate separations (>1000 nm) the liquid drag force can be modeled using a classical hydrodynamic drag force expression. For separations between the tip and substrate smaller than around 100 nm in a water medium, the force due to the effective viscosity increase of the compressed films for high tip/substrate relative velocity is comparable to the contribution of the double-layer repulsion and the van der Waals attraction. After tip/substrate contact these compressed films produce an attractive force that is a function of the liquid medium. In the DMSO medium the attractive force between tip and substrate shows an adhesive force that has at least two components indicating a multilayered structure between the tip and substrate during the tip/substrate separation. The scanning of a surface immersed in water and DMSO with a tip "in contact" produces distinct AFM images which depend on the liquid. These images show diverse symmetries and spacings between features which presumably correspond to the solvated atomic structure and are only obtained with atomic resolution for a scanning speed of ∼2 nm/s. It is possible to estimate the viscous relaxation time of the compressed layer value to be ∼250 ms from the observed resolution of substrate structures as a function of scanning speed.

Atomic force microscopy (AFM)[1] routinely provides images of a variety of hard periodic surfaces with better than nanometer resolution.[2−5] Images of fragile organic samples, including DNA, proteins, blood cells, Langmuir−Blodgett films, and polymers, have also been reported.[6−8] An important characteristic of atomic force microscopy as a nondestructive tool is the magnitude of the force applied by the probe on the surface to be imaged. Some authors suggest that the loading forces should not exceed 10^{-12} N for organic samples[9] and 10^{-9} N for crystalline surfaces.[10] The atomic force microscope operates by sensing the interaction forces between a cantilever probe and the sample surface. By using a cantilever with a spring constant much smaller than the effective spring constants of the atoms in the sample, sample damage can be minimized. However, other interaction forces such as capillary and surface forces are important in image interpretation because they may create large contact areas, even before the cantilever applies any external load to the sample. The loads generated by surface forces may cause very high pressures at the tip contact point, and the presence of these forces in the contact-mode imaging, while offering higher resolution than for noncontact imaging, may deform or damage the tip and/or the sample. In order to eliminate capillary forces and also to reduce the effect of surface forces, the acquisition of AFM images of some soft materials has been performed in aqueous solutions. There also have been claims[11,12] that atomic force microscope operation is more stable in water than in air or vacuum. In fact, any immersion medium should have a distinct effect on the dispersion force between the probe and the sample in terms of a dielectric contribution. In particular, highly polar H-bonding liquids (particularly water) are known to cause a considerable reduction (by factors of 10 or more) in the van der Waals forces with respect to those for the vacuum level. Besides that, a tip/sample combination in a liquid medium results in a more isotropic polarizable system than does the same combination in air or vacuum, with a resulting substantial reduction of the van der Waals forces.[13] It may in fact be possible, by introducing a liquid of suitable polarizability (depending on the tip/sample combination), to render the van der Waals forces negligible. This paper reports that liquids give rise to effects that may substantially modify the observed images. These effects were analyzed by measuring forces acting on the cantilever due to the presence of liquid films between the tip and the substrate.

In these experiments a commercial AFM instrument, TopoMetrix TMX2000, was used where the movement of the cantilever was detected by the conventional deflection sensor using a four-quadrant detector enabling vertical as well as lateral force measurements. A special cell was built in order to perform observations in liquid media.[14] The cell is made of PVC, and the sample is fixed at its bottom. It is moved in the *z*, *x*, and *y* directions with respect to a stationary tip. The laser beam enters and leaves the cell through a glass plate and thus does not cross the air−liquid interface, which usually is curved. The top confining surface of the solution in the cell is far

* To whom correspondence should be addressed.
† Present address: Instituto de Ciências Biológicas e Quimica, PUCCAMP, Campinas SP, Brazil.
⊗ Abstract published in *Advance ACS Abstracts,* November 1, 1997.

(1) Binnig, G.; Quate, C. F.; Gerber, C. *Phys. Rev. Lett.* **1986**, *56*, 930.
(2) Rugar, D.; Hansma, P. K. *Phys. Today* **1990**, *43*, 23.
(3) Hansma, H. G.; Bezanilla, M.; Zenhausern, F.; Adrian, M.; Sinsheimer, R. L. *Nuc. Ac. Res.* **1993**, *21*, 505.
(4) Vesenka, J.; Guthold, M.; Tang, C. L.; Keller, D.; Delaine, E.; Bustamante, C. J. *Ultramicroscopy* **1992**, *42*, 1243.
(5) Bustamente, C. J.; Vesenka, J.; Tang, C. L.; Rees, W.; Guthold, M.; Keller, R. *Biochemistry* **1992**, *31*, 22.
(6) Drake, B.; Prater, C. B.; Weisenhorn, A. L.; Gould, S. A.; Albrecht, T. R.; Quate, C. F.; Cannell, D. S.; Hansma, H. G.; Hansma, P. K. *Science* **1989**, *243*, 1586.
(7) Weisenhorn, A. L.; Hansma, P. K.; Albrecht, T. R.; Quate, C. F. *Appl. Phys. Lett.* **1989**, *54*, 2651.
(8) Sassaki, R. M.; Douglas, R. A.; Kleinke, M. U.; Teschke, O. *J. Vac. Sci. Technol. B* **1996**, *14*, 2432.
(9) Persson, B. N. *J. Chem. Phys. Lett.* **1987**, *141*, 366.
(10) Abraham, F. F.; Batra, I. P.; Ciraci, S. *Phys. Rev. Lett.* **1988**, *60*, 1314.
(11) Drake, B.; Prater, C. B.; Weisenhorn, A. L.; Gould, S. A. C.; Albrecht, T. R; Quate, C. F.; Cannell, D. S.; Hansma, H. G.; Hansma, P. K. *Science* **1989**, *243*, 1586.
(12) Weisenhorn, A. L.; Albrecht, T. R.; Quate, C. F.; Hansma, P. K. *Appl. Phys. Lett.* **1989**, *54*, 2651.
(13) Israelachvili, J. N. *Intermolecular and Surface Forces*; Academic Press: New York, 1985; Section 11.4.
(14) Weisenhorn, A. L.; Maivald, D.; Butt, H. J.; Hansma, P. K. *Phys. Rev. B* **1992**, *45*, 11226.

S0743-7463(97)00620-3 CCC: $14.00 © 1997 American Chemical Society

removed from the cantilever beam. In this geometry the displaced liquid follows a path that is perpendicular to the cantilever beam. We have obtained the best results in these measurements with very soft cantilevers, typically ~0.02 N/m (Microlever, type B, Park).

The instrument was calibrated and the measured spring constant in air (0.023 nN/nm) was found to agree with that specified by the cantilever manufacturer (0.02 nN/nm). Ethanol (>99.8%, Merck), dimethyl sulfoxide (DMSO) (>99.8%, Carlo Erba), carbon tetrachloride (CCl_4) (>99.8%, Merck), and water (Milli-Q Plus quality, resistivity = 10 MΩ cm) were introduced into the cell after the freshly cleaved mica was mounted on the *xyz* translator of the atomic force microscope. The experiments were performed at temperatures of 20 and 25 °C. Piezo-electric scanning creep effects were shown to be negligible through observations that the force vs distance measurements in air at high scanning speed (~100 μm/s) do not show hysteresis effects.

When force vs tip/sample separation curves are being generated, the cantilever support is maintained at a fixed position in the image scanning plane and the sample is moved in the perpendicular direction (*z* axis), thus moving alternately away from and toward the tip. The force vs distance curves reveal the forces on the AFM tip interacting with a sample surface in the presence of the liquid. Figure 1a shows a force vs separation curve using a Si_3N_4 tip and a mica surface immersed in water. In the previously reported curves[14,15] when the probe and sample are not in contact and the sample is approaching the tip, there are no long-range attractive or repulsive forces so there is no displacement of the straight line of the force vs tip/substrate separation curve and consequently no separation between the lines a−b and g−h. Figure 1a−c shows the force vs distance curves for various approaching velocities along the *z*-axis. Here we observe that the difference between the segments a−b and g−h for an identical initial setup position is a function of the approaching velocity [compare curves 10 μm/s (curve a) and 100 μm/s (curve c)]. This is strong evidence that imaging in a liquid medium with an atomic force microscope needs to take into consideration the liquid drag force on the tip deflection. The drag force per unit length of a cylinder with a radius R is found to be[16]

$$F = 4\pi\eta v/[1/2 - \gamma - \log(vR/4\nu)]$$

where $\gamma = 0.577$ is Euler's constant, ν is the kinematic viscosity, v is the fluid velocity relative to the cylinder, η is the dynamic viscosity, and we assume flow past an infinite cylinder with the main stream perpendicular to the axis of the cylinder, which is a good approximation even for a cantilever ~5° off the normal to the flow direction. For a liquid velocity $v = 100 \times 10^{-4}$ cm/s , $\eta =$ 0.010 02 g/(cm s), $\nu = 0.010\ 04$ cm^2/s, $l = 200$ μm, and $R = 10$ μm we obtain $F \approx 71$ pN, in good agreement with the experimental results for water (~75 pN, Figure 1c).

Another point to be observed in Figure 1a−c, which shows force vs distance curves for low scanning speeds and for water and a mica substrate, is that there is a cantilever deflection contribution due to the surface proximity ~100 nm before the sample touches the surface. This effect is indicated in Figure 1a by the region $X-Y$, which shows the apparent tip/sample contact point X, without the cantilever drag effect described in the previous

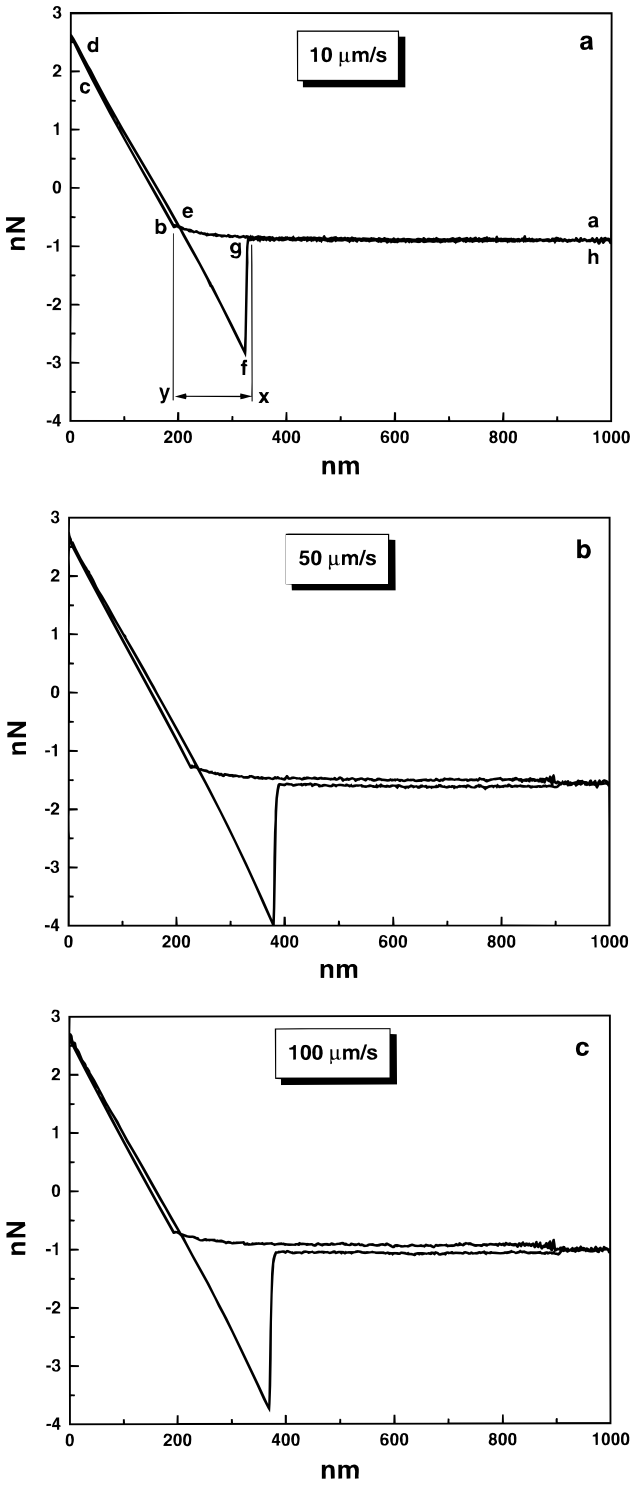

Figure 1. Observed force on the cantilever as a function of the tip/sample separation for relative velocities of (a) 10, (b) 50, and (c) 100 μm/s for a Si_3N_4 tip and a mica surface immersed in water. Section $a-b$ records the approach of the sample to the stationary tip, and point b shows a jump to contact. Section $b-c$ records the force on the cantilever as the sample continues in the same direction, while $d-c$ records the return and $e-f$ shows that a cohesion force is present and only overcome at f, when the tip suddenly returns to the equilibrium position. Section $g-h$ registers the progressive separation of the tip/sample. Spring constant = 0.02 N/m.

paragraph, and the observed contact point Y. This repulsive force is due to double-layer forces of charged surfaces in an ionic solution. The double-layer repulsion contribution has been reported[17] and it is calculated as follows:[16] For two equally charged flat surfaces the

(15) Teschke, O.; Douglas, R. A.; Prolla, T. A. *Appl. Phys. Lett.* **1997**, *70*, 1977.

(16) Landau, L. D.; Lifshitz, E. M. *Fluid Dynamics*; Pergamon Press: London, 1959; p 70.

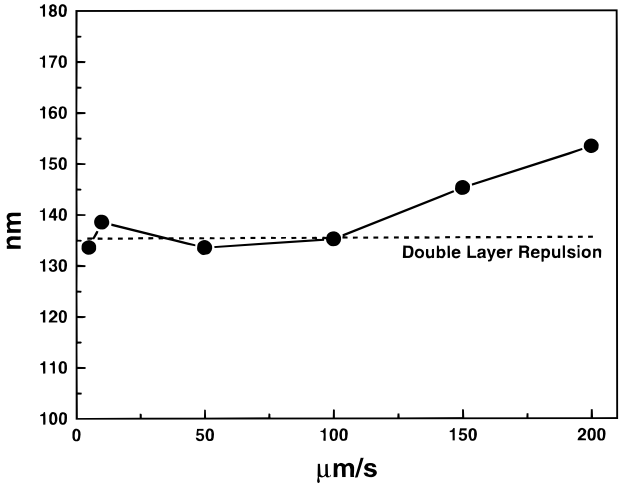

Figure 2. Separation between the apparent contact and the real contact points (*XY* in Figure 1a) as a function of the tip/sample relative velocities for a Si_3N_4 tip and a mica sample immersed in water.

repulsion decays exponentially, $\sim e^{-KZ}$, where Z is the distance between the surfaces. For low surface potentials (25 mV) $K = (ne^2/\epsilon\epsilon_0 kT)^{1/2}$ or $1/K = 0.305(1/n)^{1/2}$ nm, where n is the ionic concentration, $\epsilon = 79$, and $T = 297$ K. The characteristic length $1/K$ is called the Debye length and for low conductivity water is ~150 nm.

The length of the $X-Y$ region as a function of the relative tip/sample velocity is plotted in Figure 2, where it is possible to observe for scanning speeds up to 100 μm/s a width of aproximately 135 nm. For scanning speeds higher than 100 μm/s there is an increase of $X-Y$ with scanning speed. This increase in the repulsion force with scanning speed cannot be associated with the double-layer repulsion, which is independent of the scanning speed. We are concerned here with the solid−liquid interface, where the disordered liquid state competes with the ordering potential of the surface. Recently methods were devised to measure the shear response of liquid films so thin that their thicknesses approach molecular dimensions.[18,19] In this rapidly developing area, most studies have observed a loss of fluidity and a subsequent increase in dynamic friction when the film thickness is in the range of 1−3 molecular dimensions. Here we observe an increase of the total force acting on the cantilever, which included the double-layer repulsion plus a velocity dependent component, when the film thickness is ~100 nm. Since this last contribution is scanning speed dependent, it was associated with a viscosity increase, as observed for molecular dimension films. This observed effective viscosity of the compressed film suggests considerable distortion of the dynamic structure of the liquid between the tip and the substrate.[20] The same effect is observed for DMSO where the velocity dependent contribution starts at ~5 μm/s compared to 100 μm/s in water and at high speeds (~100 μm/s) shows an increase in the repulsive force by a factor of 2.

The presence of a compressed liquid layer between the tip and the substrate in water even after the "contact" is made with the sample is confirmed by the following:

(1) The slope of the line $b-c$ in Figure 1a is variable, which indicates that the width of the layer between the tip and substrate decreases as the force imposed by the substrate displacement increases. For samples scanned in air this slope is only a function of the elasticity and plasticity of the sample. This is not a conclusive result but is an indication of the presence of the compressed film.

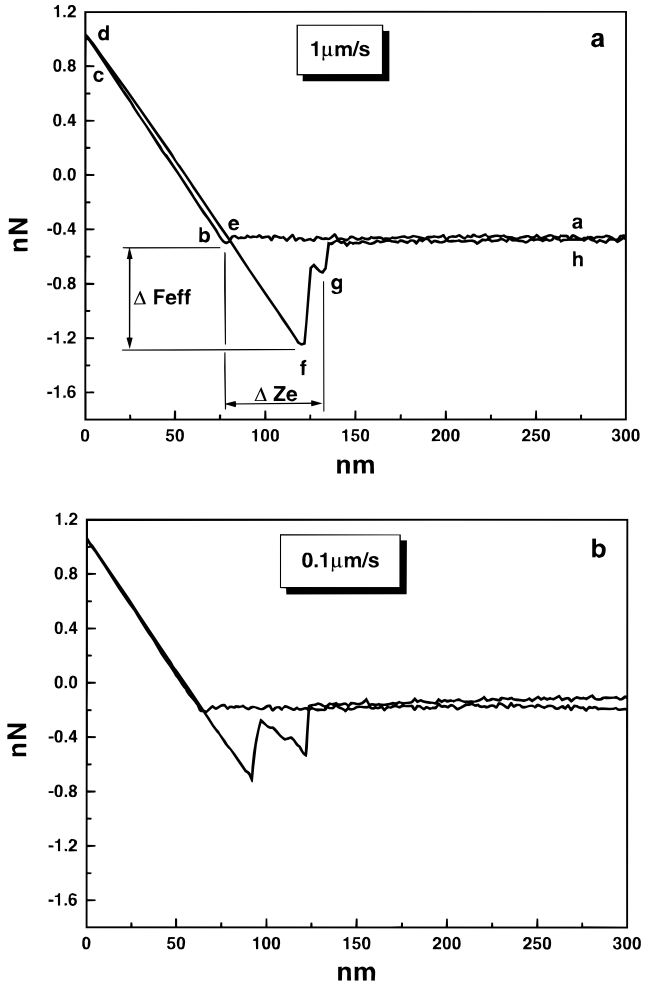

Figure 3. Force vs separation curves (as in Figure 1) for a Si_3N_4 tip and a mica sample immersed in DMSO for relative velocities of (a) 1.0 and (b) 0.1 μm/s. Spring constant = 0.02 N/m; factor conversion = 0.117 N/A.

(2) Segment $e-f$ in Figure 1a records the motion of the cantilever from its neutral deflection position as it is deflected downward (therefore representing an adhesive force) until the spring force of the cantilever exceeds the adhesive force when the tip breaks away from the surface. The segment $f-g$ shows the jump of the cantilever away from the surface, which occurs when the cantilever force exceeds the adhesive forces; the force at point f is the maximum adhesive force between the probe and the sample. The separation distances between contact and separation points in Figure 1a−c (during sample retraction) are 137, 159, and 182 nm, respectively. The corresponding tip/sample adhesion forces are 2.0, 2.3, and 2.7 nN. For measurements made in vacuum this force increase was associated with the deformation of tip and/or substrate at the contact region. Here a distortion of the liquid dynamic structure is suggested.[20] Initially the effect of dynamic friction was investigated in a highly polar protic solvent. Now these effects are investigated in highly polar but dipolar aprotic DMSO, resulting in quite distinct solvation properties.

(3) Initially the forward and return lines in Figure 3 are observed to be coincident. This is a consequence of the fact that the DMSO viscosity is 0.02 g/cm·s and the

(17) Hoh, J. H.; Cleveland, J. P.; Prater, C. B.; Revel, J. P.; Hansma, P. K. *J. Am. Chem. Soc.* **1992**, *114*, 4917.
(18) Horn, G. R.; Israelachvili, J. N. *J. Chem. Phys.* **1981**, *75*, 1400.
(19) Thompson, P. A.; Robbins, M. O. *Phys. Rev. A* **1990**, *41*, 6830.
(20) Hartmann, U. *Phys. Rev. B* **1991**, *43*, 2404.

scanning speed in Figure 1c is 100 μm/s while that in Figure 3a is 1 μm/s, which gives a drag force factor 82 times smaller for DMSO than for water shown in Figure 1.

The sharp break away at point *f* shown in Figure 1a−c is not a universal response. For a DMSO medium a distinctive effect was observed. If the adhesive interaction can be characterized as being viscoelastic, the probe may not break away from the surface abruptly but may produce a much more gradual and smooth or even a stick−slip response. This is shown in Figure 3 for mica immersed in DMSO. Here we observe that the pull-off process occurs in two steps: the first decrease in the adhesive force seems to correspond to a deformation of the residual thin liquid films adherent to both the mica and the tip surfaces, and the second decrease corresponds to the rupture of these films and the complete separation of the tip from the substrate. The presence of this adherent liquid film and its plasticity are responsible for this two-step breaking away from the interface.

The relative intensity of the two breaks in the tip/sample separation curves depends on the scanning velocity, as is seen by a comparison of parts a and b of Figure 3. For higher tip/sample relative velocities the two-step nature is less apparent. It is also evident that the *z* coordinate is different when the tip and sample are at their closest approach and when there is a rupture. This distance is shown as Δz_e in Figure 3a. At low scanning speeds the relative tip/sample velocity has little influence on this distance, as can be seen by comparing parts a and b of Figures 3. These effects can be studied to obtain information on the structure and viscoelastic properties of adsorbed layers on the tip and/or sample surfaces.

The van der Waals attraction force is usually thought to be responsible for the adhesion force; consequently, the van der Waals forces between the surface and the tip were calculated for water, ethanol, and DMSO. The calculated van der Waals forces for silicon nitrite/solvent/mica, considering a tip/substrate distance of 0.1 nm, are −2.21 nN for water, −0.43 nN for DMSO, and −1.10 nN for ethanol. The calculated adhesive forces decrease in the following sequence: water > ethanol > DMSO; however, the measured adhesion forces are −2.05 nN for water, −0.78 nN for DMSO, and negligible for ethanol. This fact may be explained if we consider that the "contact" distance between the tip and the surface, and therefore the solvation layer, is smaller for DMSO than for ethanol. This assumption is also consistent with the presence of a compressed liquid film remaining between the tip and the substrate even after contact.

The effect of the structure and viscoelastic properties of the compressed film on the observed images of the surface was then investigated. Measurements were made of the structure of a 0.5 cm^2 freshly cleaved mica surface covered by a small amount (20 μL) of Milli-Q Plus water, which should have quickly equilibrated with the mica at room temperature. Relatively stable imaging was possible within a few minutes after adding the liquid.

The effect of imaging a surface within different liquid media is demonstrated in Figure 4, where images of mica samples obtained (a) in air, (b) immersed in DMSO, and (c) in water at 25 °C are presented. The patterns observed are clearly dependent on the immersion medium. These measurements were performed at low scanning speed (2 nm/s). For comparison, the models of images of the mica surface built from X-ray data are shown in Figure 5.

The pattern observed in Figure 4a corresponds roughly to the original position of the K^+ ions on the mica surface: the clearer spots are located along almost parallel lines separated by 0.54 nm, and the distance between two

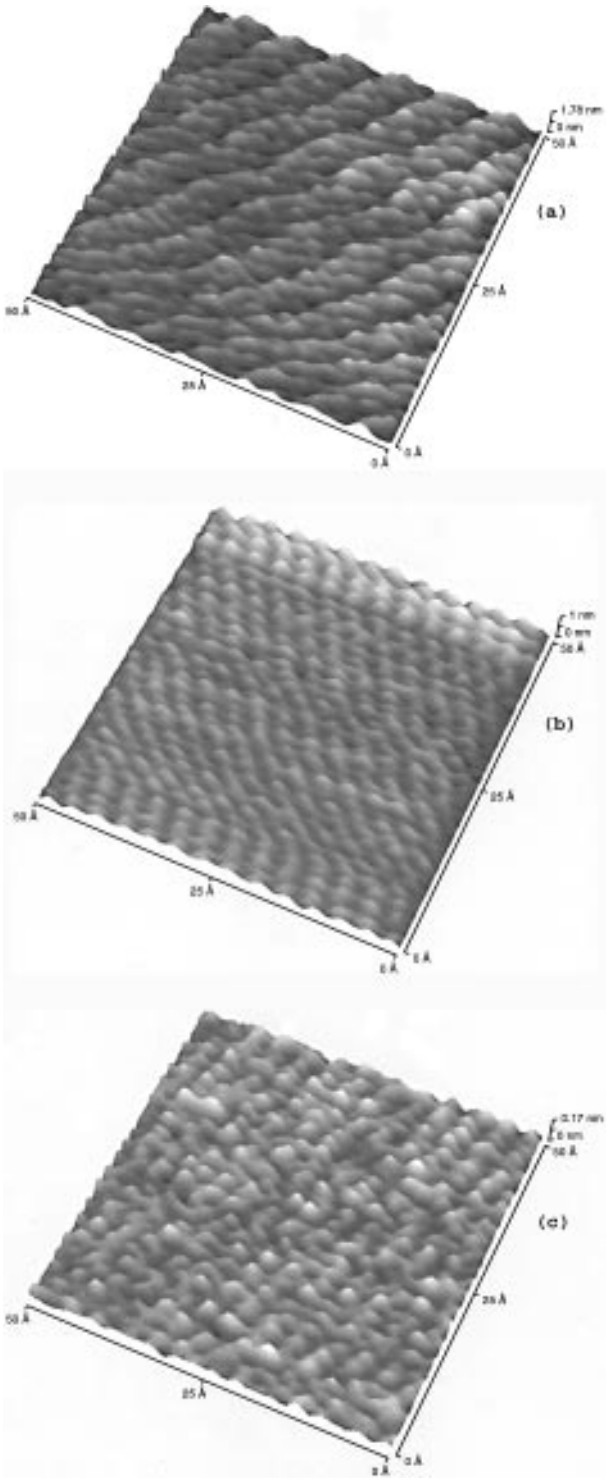

Figure 4. Image of the same mica surface when the tip/sample system is (a) in air and immersed in (b) DMSO and (c) water at 25 °C (scanning speed 2 nm/s).

clearer spots along the line is 0.235 nm. The measured angle between these two directions is 38°. The region imaged has a number of clearer spots that correspond to a density of 4.4×10^{14} spots/cm^2. These data are shown in Table 1 and are compared with those extracted from Figure 5a in Table 2. Observe that this image was obtained in air at 20 °C with a humidity of 50%; consequently, we cannot exclude the possibility that the clearer spots correspond to the position of the K^+ ions with water molecules arranged around them.

A completely different pattern is obtained from samples immersed in DMSO (Figure 4b and Table 1). These results

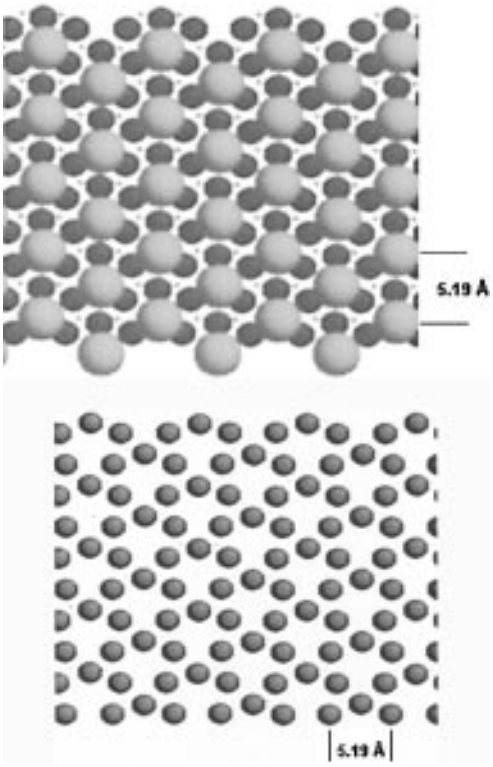

Figure 5. Theoretical configurations of atoms of K and O at the surface of a mica sample: (a) top layer potassium (indicated by large whitish circles); and (b) top layer oxygen.

Table 1

observed mica surface	density (spots/cm^2)	separation of lines (nm)	spacing of features (nm)	angle, θ
air, 20 °C, 50% humidity	4.4×10^{14}	0.54	0.235	38
DMSO, 20 °C	10.5×10^{14}	0.44	0.26	65
water, 25 °C	13×10^{14}	0.44	0.255	60

Table 2

modeled mica surface	density (spots/cm^2)	separation of lines (nm)	spacing of features (nm)	angle, θ
O atoms occupying the upper layer	12×10^{14}	0.519	0.26	60
K atoms occupying the upper layer	4×10^{14}	0.448	0.26	30

therefore suggest that when mica is immersed in DMSO, the K^+ ions desorb from its surface and remain in solution completely solvated by the highly dipolar aprotic solvent molecules within the double-layer, thus leaving behind an almost nonsolvated negatively charged surface which reveals the position of the O^- ions.

The images obtained in water at 25 °C and shown in Figure 4c resemble that of Figure 5b: in both images the distance between two consecutive lines of clearer spots is 4.4 Å and their number corresponds closer to 12×10^{14} spots/cm^2 than to 4×10^{14} spots/cm^2. In this case it should be noted that the K^+ ions initially held on the mica surface in the high-resistivity water (10 MΩ cm, 7×10^{-6} M 1:1 electrolyte at pH ~ 6) should be at least partially H_3O^+ ion-exchanged. Considering that the solvent volume of the cell was 300 mL and the mica exposed area was 1.13 cm^2, if all K^+ ions on the mica surface were exchanged into solution, the K^+ concentration would be about 8.3×10^{-8} M, almost two orders smaller than the calculated concentration of the H_3O^+ present in the solution. Consequently these images probably correspond to the mica surface covered with the H_3O^+ ions arranged near the O^- ions of the substrate.

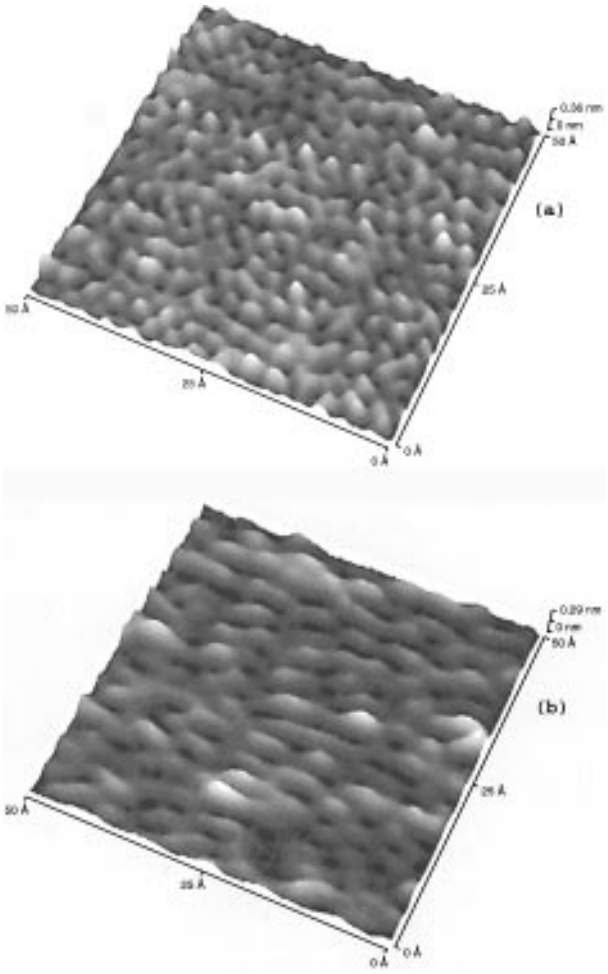

Figure 6. Image of the same mica surface in water at 25 °C when the scanning speed is (a) 2 and (b) 5 nm/s.

A quantitative measurement of the viscoelastic properties of the compressed films is difficult as is the assessment of the differences between the two adhesion curves shown in parts a and b of Figure 3. However an increase in the scanning speed to 5 nm/s results in an almost complete loss of the image resolution, as shown in Figure 6. The image obtained with the scanning speed 2 nm/s (Figure 6a) shows atomic resolution while the one obtained with a 5 nm/s scanning speed shows much larger periodic features. This is the consequence of the fact that the viscous force in the film between the tip and the surface damps the vertical movement of the tip which is responsible for the atomic resolution. If we consider that the periodicity of the mica "atoms" is approximately ~0.5 nm and use the scanning speed for which there is a substantial decrease in the resolution, we obtain the relaxation time 250 ms. This value is estimated assuming an exponential decay of the vertical tip motion $z = z_0 e^{-t/t_0}$, where z_0 is the vertical height of the sample structure and t_0 is the relaxation time, and observing the resolution as a function of the scanning speed. The relaxation time (t_0) is in agreement with the previously measured values[21] and reflects the collective motions induced by the tip/substrate confinement. This collective motion induced by the confinement is in agreement with the fact that adhesion forces were obtained for water and DMSO, which are highly polar solvents, which show ordering close the substrate interface while in the case of less polar solvents

(21) Hu, H.; Carson, G. A.; Granick, S. *Phys. Rev. Lett.* **1991**, *66*, 2758.

like methanol, ethanol, and 2-propanol this effect goes undetected.

In conclusion it was shown experimentally that for high approaching substrate/tip velocities there is a viscous drag force which acts on the cantilever cylinder and is proportional to the approaching velocity. When the tip gets close to the liquid−substrate interface, a distinctive viscous drag force is measured. This force is associated with the compression of the liquid between the substrate and the tip which is added to the double-layer repulsion and the van der Waals attractions for scanning speeds above 100 μm/s. It is measured for tip/substrate separations of ∼100 nm in water, a distance much larger than the previously reported values for a few molecular layers. The presence of the compressed film between the tip and the substrate is confirmed by force vs distance curves which clearly show a force dependence on approaching velocity attributed to distortion of the liquid dynamic structure due to compression.[19] The liquid layers remaining between the surface and the tip produce a force that depends on the liquid medium. Atomic-scale images produced by the AFM typically show features depending on the liquid which do not correspond to the presumed atomic-scale structure and also show the complete loss of the image resolution for the scanning speed 5 nm/s. This indicates that the viscosity of the compressed film plays a determining role in the resolution of the scanned images, since atomic features are obtained for scanning speeds of ∼2 nm/s, which is far too small to have relevant contributions due to the other effects described. It is also possible to estimate the viscous relaxation time of the compressed layer value to be ∼250 ms from the observed resolution of substrate structures as a function of scanning speed.

Acknowledgment. The authors would like to thank M. C. Santos for stimulating discussions and L.O. Bonugli for technical assistance. This work was supported by FINEP and CNPq Grant 523.268/95-5.

LA970620M